Light Scattering Study of Semiflexible Polymer Solutions. 1. Dilute through Semidilute Solutions of Poly(*n*-hexyl isocyanate) Dissolved in Dichloromethane

Yuji Jinbo, Takahiro Sato,* and Akio Teramoto

Department of Macromolecular Science, Osaka University, Toyonaka, Osaka 560, Japan

Received April 4, 1994; Revised Manuscript Received July 27, 1994®

ABSTRACT: Dilute through semidilute solutions of a semiflexible polymer, poly(*n*-hexyl isocyanate) (PHIC), dissolved in a good solvent, dichloromethane (DCM), were studied by static light scattering as well as by sedimentation equilibrium. The solutions showed the following characteristic features, which were distinct from those of flexible polymer–good solvent systems. (1) The second virial coefficient was independent of the molecular weight. (2) The reduced third virial coefficient was much smaller than that for a flexible polymer in a good solvent. (3) The concentration dependences of the osmotic compressibility ($\partial c/\partial \Pi$) and correlation length ξ did not obey the scaling law nor the prediction of the renormalization group theory that was successful for flexible polymer–good solvent systems. Except for the correlation length results, the above features were favorably compared with a scaled particle theory including a weak attractive interaction. The present study is an advance on a previous work (Sato, T.; Teramoto, A. *Mol. Cryst. Liq. Cryst.* **1990**, *178*, 143) in that thermodynamic properties of semiflexible polymer solutions are understood on a more realistic molecular basis taking an attractive potential into account.

1. Introduction

The monomer-unit pair distribution function is one of the most basic quantities for a polymer solution, which describes its local structure.[1,2] The pair distribution function consists of the intramolecular and intermolecular distribution functions. In dilute solutions, only the former distribution function is important, but in semidilute solutions, where neighboring polymer chains overlap each other, both the intramolecular and intermolecular distribution functions play important roles. In general, these distribution functions are determined by the intramolecular and intermolecular excluded volume effects along with the connectivity of individual chains.

The intramolecular distribution function of a flexible polymer chain in a good solvent is perturbed by the intramolecular excluded volume effect. In the dilute regime, this excluded volume effect makes the intramolecular distribution function broader than that in the unperturbed state. As the polymer concentration increases, however, the intermolecular excluded volume effect becomes important to change both the intermolecular and intramolecular distribution functions. Owing to this effect, different polymer molecules repell each other, and the intermolecular (radial) monomer distribution function has a minimum around the center-of-mass position of the chain under consideration. At the same time, the intermolecular excluded volume effect tends to screen out the intramolecular excluded volume effect. As a result, the intramolecular monomer distribution becomes narrower with increasing polymer concentration and reaches the unperturbed one in bulk. Therefore the total monomer-unit pair distribution function for a flexible polymer solution is expected to exhibit a complex polymer concentration dependence due to cooperative effects of the intramolecular and intermolecular excluded volumes. The local monomer distribution in a flexible polymer solution was favorably compared with renormalization group theories into which were incorporated the above *intra- and intermolecular* excluded volume effects.[3–6]

In contrast to flexible polymers, a stiff-chain or semiflexible polymer with a relatively small Kuhn statistical segment number is known not to be perturbed by the intramolecular excluded volume effect even in a good solvent, because of a negligible probability of the collision among segments within one chain far separated along the chain contour.[7,8] This fact indicates that the excluded volume screening effect may not be important in semidilute solutions of stiff-chain polymers, although there are not direct measurements of the dimensions of stiff-chain polymers in such solutions. From these considerations, we may expect that the polymer chain stiffness plays an important role in the monomer-unit distribution function of the local structure of semidilute polymer solutions.

For scattering experiments of semidilute solutions of stiff-chain polymers, we may face the following general experimental difficulties: (1) preparation of stiff polymer samples with a narrow molecular weight distribution is not an easy task; (2) many stiff polymers have poor solubility in usual solvents and easily form aggregates or microgels in solution. Owing to these experimental difficulties, experimental studies on the local structure in semidilute solutions of stiff polymers by light scattering have been quite meager so far. Only recently, DeLong and Russo[9] made a static (and also dynamic) light scattering study on α-helical poly(γ-benzyl L-glutamate) (PBLG) solutions over a wide concentration region. However, it is uncertain that their data are free from the nonideality due to aggregates over the polymer concentration range they examined.

In the present study, we chose poly(*n*-hexyl isocyanate) (PHIC), which has a persistence length of 21 nm in dichloromethane (DCM).[10] The fractionation of this polymer can be made rather effectively and the solubility is quite good for some common organic solvents.[10–12] Using well-fractionated PHIC samples dissolved in DCM, we carried out a static light scattering study over wide ranges of polymer concentration and molecular weight. From dilute solution data, we obtained the radius of gyration, second virial coefficient, and intramolecular interference factor. On the other hand, we obtained, from dilute through semidilute solution data, the correlation length ξ and osmotic compressibility ($\partial c/\partial \Pi$) (c is the polymer

® Abstract published in *Advance ACS Abstracts*, September 1, 1994.

0024-9297/94/2227-6080$04.50/0

Table 1. Characteristics of PHIC Samples Used for the Light Scattering and Sedimentation Equilibrium Experiments

sample	$M_w/10^4$	$A_2/10^4$ [a]	$\langle S^2\rangle^{1/2}$/nm	$[\eta]/(\mathrm{cm^3\ g^{-1}})$	N	M_w/M_n [b]	$c^*/(10^{-3}\ \mathrm{g\ cm^{-3}})$ [c]
K-3	11.1	6.10	26.6	268	3.57	1.05	2.34
M-1	18.0	6.24	35.6	435	5.79	1.05	1.58
I-2	25.3	6.49	44.6	597	8.14	1.10	1.13
C-3	34.2	6.28	52.3	749	11.0		0.948
J-2	48.1	6.46	64.2	1020	15.5		0.721
F-2	72.4	5.97	80.5	1410	23.3		0.550
V-1-2	106	6.23	97.9	1880	34.1		0.448

[a] In units of $\mathrm{cm^3\ mol/g^2}$. [b] Determined from GPC. [c] The overlap concentration calculated by $c^* = 3M_w/4\pi N_A\langle S^2\rangle^{3/2}$.

mass concentration, and Π is the osmotic pressure) as functions of c. The last quantity was also obtained by sedimentation equilibrium. This paper presents these experimental results for the PHIC–DCM system in comparison with the corresponding results for flexible polymer solutions.

In a previous paper,[13] $(\partial c/\partial\Pi)$ data of the PHIC–DCM system obtained by sedimentation equilibrium were shown to be favorably compared with the scaled particle theory for hard spherocylinder solutions. In the present paper, we compare both $(\partial c/\partial\Pi)$ and the second virial coefficient of the same system obtained by light scattering and sedimentation equilibrium with a scaled particle theory which is modified by taking into account a weak attractive interaction between polymers.

2. Experimental Section

2.1. Samples. Poly(n-hexyl isocyanate) (PHIC) samples were prepared by polymerization of n-hexyl isocyanate (Kanto Chemical Co., Ltd.) followed by fractionation according to the method described before.[10] The only difference from the previous method was to use benzene instead of carbon tetrachloride as the solvent for fractionation. Seven fractionated PHIC samples were used for the light scattering experiment, and two among them were chosen for the sedimentation equilibrium experiment. The ratios of the weight-average to number-average molecular weights M_w/M_n determined from GPC were equal to or less than 1.1 for the three lowest molecular weight samples examined (cf. Table 1). This value indicates that the fractionation was done successfully. In the following analysis, all the PHIC samples used will be regarded as monodisperse.

2.2. Light Scattering. Intensities of the scattered light from DCM solutions of PHIC at 20 °C were measured on a Fica 50 automatic light scattering photogoniometer. The incident light of 436 and 546 nm was vertically polarized, and the scattering intensity was measured without an analyzer, except for the depolarization measurements mentioned below. The photogoniometer was calibrated using benzene as a reference material.[11] Cylindrical light scattering cells with an inner diameter of 15 mm with a stopper were used; the cells were directly spun in a centrifuge for optical clarification.

Solutions with the concentration c lower than ca. 5 times the overlap concentration c^* (cf. eq 3) as well as the solvent were filtrated through Millipore filters with suitable pore sizes directly into the light scattering cells and centrifuged at 10 000 rpm for 2–3 h in a Sorvall RC-5C centrifuge. Then the cell was set on the photogoniometer without disturbance and subjected to scattering intensity measurements. On the other hand, more concentrated solutions were prepared in the following way. First, solutions with $c \approx 5c^*$ were filtrated through suitable Millipore filters directly into the light scattering cells. Then the solutions in the cells were gently heated below the boiling temperature to evaporate the solvent slowly, resulting in moderately concentrated solutions. Finally, the solutions in the cells were centrifuged and subjected to the light scattering measurement.

In this and forthcoming papers, the light scattering intensity is expressed in terms of the structure factor $\hat{S}(k)$ defined by

$$\hat{S}(k) \equiv \frac{R_\theta}{KcM_0} \tag{1}$$

where R_θ is the excess Rayleigh ratio at the scattering angle θ conventionally used in the light scattering experiment for dilute polymer solutions, K is the optical constant, c is the polymer mass concentration, and M_0 is the molar mass of the monomer (=127); the argument k of $\hat{S}(k)$ is the absolute value of the scattering vector given by $k = (4\pi n/\lambda_0)\sin(\theta/2)$, where n is the refractive index of the solution and λ_0 is the wavelength of light in vacuum.

The osmotic compressibility $(\partial c/\partial\Pi)$ (at constant temperature T and solvent chemical potential) and the correlation length ξ were estimated as functions of c using the equation[6]

$$\hat{S}(k)^{-1/2} = \left[\frac{RT}{M_0}\left(\frac{\partial c}{\partial\Pi}\right)\right]^{-1/2}\left[1 + \frac{1}{2}\xi^2k^2 + O(k^4)\right] \tag{2}$$

where R is the gas constant.

The optical anisotropy of the PHIC molecule in DCM was checked by measuring depolarized scattering intensities for dilute and semidilute solutions with sample K-3 (cf. Table 1) using the vertically polarized incident light and the analyzer oriented to the horizontal direction. The depolarized structure factor $\hat{S}_{Hv}(k)$ calculated from the intensities with eq 1 was almost independent of c and k at $c < 0.03\ \mathrm{g/cm^3}$, and the value of $\hat{S}_{Hv}(k)/\hat{S}(0)|_{c=0}$ was as small as ca. 4.4×10^{-3}. This value indicates that the optical anisotropy correction to the molecular weight is less than 1%. Therefore all the light scattering data were analyzed without correcting for the optical anisotropy. Murakami et al.[11] reported a similar small optical anisotropy for PHIC in n-hexane.

DeLong and Russo[9] reported an increase of the depolarization ratio $\rho\ [\equiv\hat{S}_{Hv}(k)/(\hat{S}(k) - \hat{S}_{Hv}(k))]$ with increasing c for the system PBLG–dimethylformamide (DMF). However, the concentration dependence of ρ is affected not only by a change of $\hat{S}_{Hv}(k)$ but also by a change of $\hat{S}(k)$ with c. (In fact, an increase of ρ with c was obtained from our $\hat{S}_{Hv}(k)$ and $\hat{S}(k)$ data of the PHIC–DCM system). The optical anisotropy of a polymer solution should be expressed by $\hat{S}_{Hv}(k)$ rather than by ρ.

The specific refractive index increment $(\partial n/\partial c)$ was measured at 20 °C by a modified Schultz–Cantow differential refractometer. At $c < 0.04\ \mathrm{g/cm^3}$, the excess refractive index of the solution over the solvent linearly increased with c at both 436 and 546 nm wavelength. From those results, $(\partial n/\partial c)$ was estimated to be $0.0698\ \mathrm{cm^3/g}$ at 436 nm and $0.0659\ \mathrm{cm^3/g}$ at 546 nm irrespective of c within the range of c where the light scattering measurements

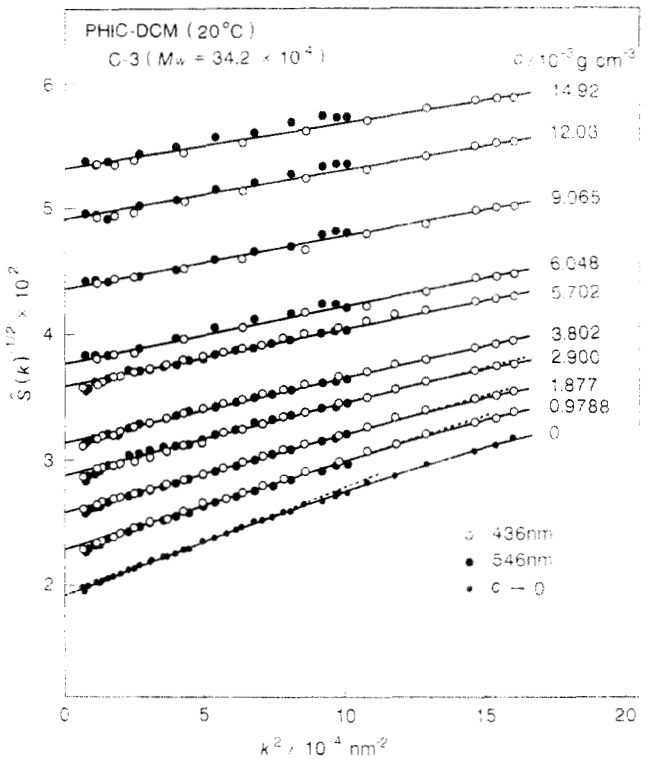

Figure 1. Plot of $\hat{S}(k)^{-1/2}$ vs k^2 for dilute through semidilute solutions of sample C-3 at 20 °C.

were made ($c < 0.03$ g/cm^3). Light scattering data from dilute through semidilute solutions were analyzed with these values of $(\partial n/\partial c)$.

The light scattering experiment is very sensitive to imperfect solubility or the existence of a tiny amount of aggregates in the test solution, and this nonideality may provide serious errors in the light scattering results of the osmotic compressibility $(\partial c/\partial \Pi)$, the correlation length ξ, etc. Since stiff polymer solutions often have poor solubility, it is very important to check whether the test solution of PHIC is free from aggregates. This check is done by comparing $(\partial c/\partial \Pi)$ data obtained from light scattering with those from sedimentation equilibrium (see below).

2.3. Sedimentation Equilibrium. The osmotic compressibility for binary solutions can be determined also by the sedimentation equilibrium method, which is not so sensitive to a tiny amount of aggregates. If the test solution is free from aggregates, it is imperative that $(\partial c/\partial \Pi)$ obtained from light scattering agree with that from sedimentation equilibrium. Thus this comparison is a crucial check for the reliability of the light scattering results.

The concentration distribution of PHIC solutions at 20 °C under a centrifugation field was determined on a Beckman Spinco Model E ultracentrifuge using the Rayleigh interference method for $c < 5 \times 10^{-2}$ g/cm^3 and using the schlieren method for higher concentration. From our data of $(\partial n/\partial c)$ mentioned above combined with the results of Itou et al.[12] measured up to $c = 0.28$ g/cm^3, we obtained an empirical equation $(\partial n/\partial w) = 0.0874 - 0.0551w$ (w is the weight fraction of PHIC) for 546 nm wavelength light. This equation for $(\partial n/\partial w)$ as well as Itou et al.'s result[12] for the partial specific volume were used in the data analysis. The detailed procedure of the analysis is described in ref 12.

3. Results

3.1. Structure Factor. Figure 1 shows plots of $\hat{S}(k)^{-1/2}$ vs k^2 for the dilute through semidilute solutions of sample C-3 at 20 °C. Extrapolating this plot to the zero k, we determined $\hat{S}(0)$, which is equal to $(RT/M_0)(\partial c/\partial \Pi)$ (cf. eq 2). In Figure 2, unfilled circles show the polymer mass concentration c dependence of $\hat{S}(0)^{-1}$ obtained in this way for six PHIC samples. (The data points for sample I-2 obtained from light scattering are not displayed in Figure 2 for clarity of the figure.) On the other hand, filled circles in the same figure for samples K-3 and C-3 represent the results of $(M_0/RT)(\partial \Pi/\partial c)$ obtained from sedimentation equilibrium. It can be seen that both light scattering and sedimentation equilibrium experiments provide consistent results for the two samples.

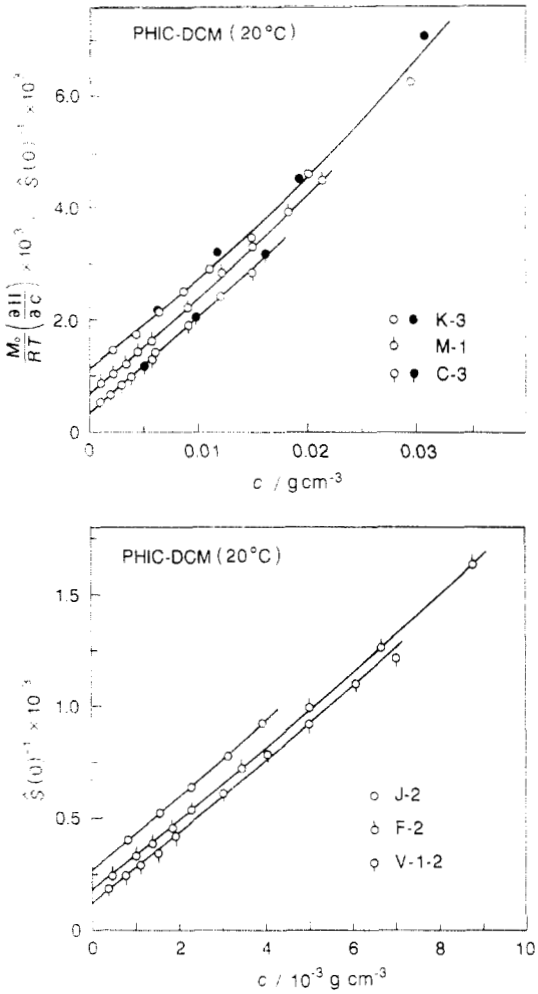

Figure 2. Polymer mass concentration c dependence of $(M_0/RT)(\partial \Pi/\partial c)$ $[\equiv \hat{S}(0)^{-1}]$ for six PHIC samples: unfilled circles, data obtained from light scattering; filled circles, data for samples K-3 and C-3 obtained from sedimentation equilibrium.

However, at higher concentrations as shown by the arrows in Figure 3 for sample K-3, light scattering gives lower $(M_0/RT)(\partial \Pi/\partial c)$ than sedimentation equilibrium. Furthermore, the plot of $\hat{S}(k)^{-1/2}$ vs k^2 at such high concentrations sometimes exhibited a downturn at very small k. This experimental nonideality indicates the presence of a tiny amount of aggregates in these solutions with the high concentrations. Therefore we will discard the light scattering data at such high polymer concentrations in the following analysis.

The weight-average molecular weight M_w and the second virial coefficient A_2 for each sample were obtained from the intercept and initial slope of the curve indicated in Figure 2. The mean square radius of gyration $\langle S^2 \rangle$ at infinite dilution was determined from the initial slope and the intercept of the plot of $\hat{S}(k)^{-1/2}$ vs k^2 at $c = 0$ as indicated by the small filled circles in Figure 1. Table 1 lists the M_w,

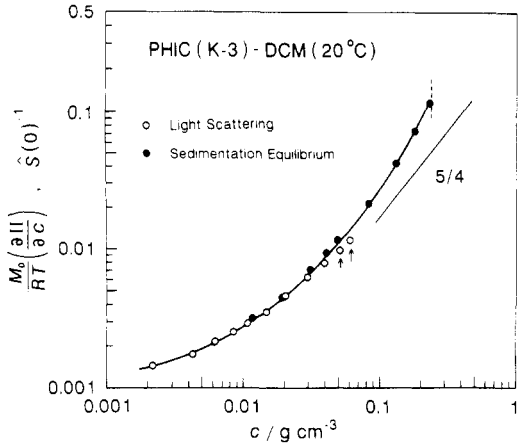

Figure 3. Double-logarithmic plot of $(M_0/RT)(\partial\Pi/\partial c)$ vs c for sample K-3 over a wide concentration range: filled circles, data from sedimentation equilibrium; unfilled circles, data from light scattering; vertical dotted segment, the isotropic–nematic phase boundary concentration c_I.

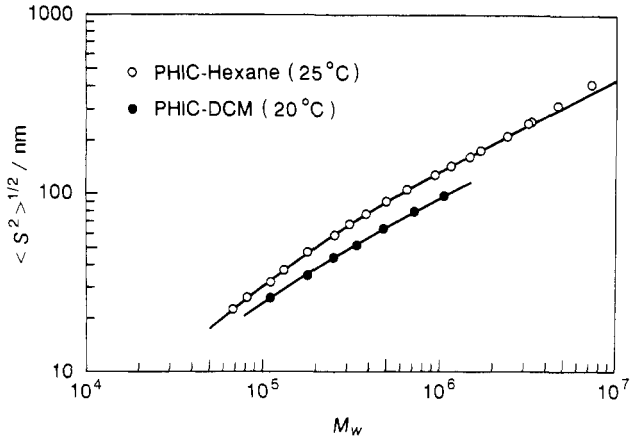

Figure 4. Double-logarithmic plot of $\langle S^2\rangle^{1/2}$ vs M_w for PHIC: filled circles, data in 20 °C DCM; unfilled circles, data in 25 °C n-hexane.[11]

A_2, and $\langle S^2\rangle^{1/2}$ results for seven PHIC samples obtained in this way.

The last column of Table 1 gives the overlap mass concentration c^* for each sample. This concentration was estimated by the equation

$$c^* = 3M_w/4\pi N_A\langle S^2\rangle^{3/2} \quad (3)$$

where N_A is the Avogadro constant. This concentration is quite low because of the rather extended conformation of PHIC. The ratios c/c^*, which express the degree of overlap of the chains in solution, range from 1.01 to 15.4 for the solutions displayed in Figure 1.

3.2. Molecular Weight Dependences of the Radius of Gyration and Second Virial Coefficient. Figure 4 shows a double-logarithmic plot of $\langle S^2\rangle^{1/2}$ vs M_w for PHIC in DCM, where filled circles represent the experimental data. The data points follow a slightly convex curve with the slopes 0.60 and 0.52 in the lower and higher molecular weight regions, respectively. These slopes manifest the stiff-chain nature of PHIC in DCM. Unfilled circles in Figure 4 represent $\langle S^2\rangle^{1/2}$ data of PHIC in n-hexane obtained by Murakami et al.[11] It can be seen that the PHIC chain takes a smaller dimension in DCM than in n-hexane, which confirms the finding of Itou et al.[10]

Figure 5 shows a double-logarithmic plot of A_2 against M_w for PHIC in DCM (filled circles) and in n-hexane (unfilled circles); the data in the latter solvent were obtained by Murakami et al.[11] These results of A_2 indicate

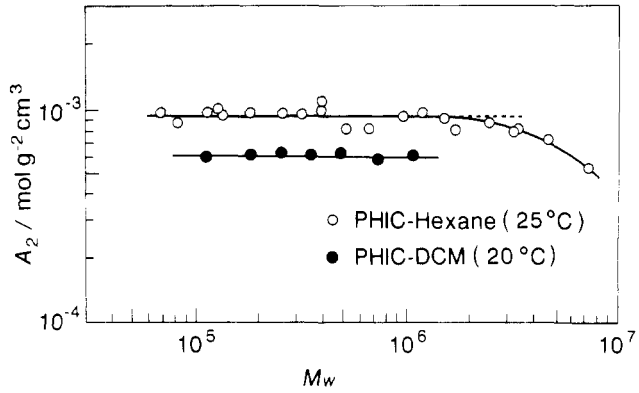

Figure 5. Double-logarithmic plot of A_2 against M_w for PHIC (same symbols as in Figure 4).

that both DCM and n-hexane are good solvents for PHIC but that n-hexane is a better solvent than DCM. The variation of A_2 for this polymer with solvent implies that the intermolecular potential may not be purely the hard-core type determined by its structure but contains an attractive type depending on solvent.

It is important to note that A_2 of PHIC is independent of M_w in both solvents for M_w below ca. 1×10^6. This behavior is in contrast with A_2 for flexible polymers in good solvents, where A_2 is a decreasing function of M_w.[15]

3.3. Concentration Dependences of the Osmotic Compressibility and Correlation Length. The concentration dependence of the osmotic compressibility $(\partial c/\partial\Pi)$ obtained from light scattering has already been shown in Figure 2. The data points for each sample follow a slightly upswing curve, which indicates that the system has a small positive third virial coefficient A_3. From the Bawn plot[14] constructed with the data shown in Figure 2, the reduced third virial coefficient g $(\equiv A_3/A_2^2M_w)$ was estimated to be 0.01_5 for sample C-3. This value is much smaller than g for flexible polymer–good solvent systems (0.2–0.5).[15] Murakami et al.[11] showed that $\hat{S}(0)$ of the PHIC–n-hexane system gives linearity in the plot of $\hat{S}(0)^{-1}$ vs c rather than in the plot of $\hat{S}(0)^{-1/2}$ vs c in the range of $c < 6c^*$. This demonstrates that g of PHIC in n-hexane is also very small.

As mentioned in section 3.1, the light scattering experiment could not provide accurate results of $(\partial c/\partial\Pi)$ for solutions with higher concentrations due to the presence of a tiny amount of aggregates (cf. Figure 3). On the other hand, sedimentation equilibrium is not so sensitive to a small amount of aggregates. Since DCM solutions of PHIC are clear up to the critical concentration c_I where the nematic phase starts forming, we can expect that sedimentation equilibrium for the solutions gives accurate $(\partial c/\partial\Pi)$ data even at such high concentrations. Thus in Figure 3 we have combined the light scattering data at relatively low concentrations with high concentration sedimentation equilibrium data to cover the entire range in isotropic solutions.

Figure 3 shows the double-logarithmic plot of $(M_0/RT) \times (\partial\Pi/\partial c)$ vs c for sample K-3 up to the vicinity of c_I (=0.24 g/cm^3). The data points follow a curve with a positive curvature. This curve has no linear region in the higher concentration region, and moreover the slope of the curve exceeds 5/4 in the vicinity of c_I. These results indicate that the scaling law for flexible polymer–good solvent systems[6,16] does not hold in the PHIC–DCM system. A similar concentration dependence was observed for sample C-3 and also by Itou et al.[12] for other PHIC samples in the same solvent condition.

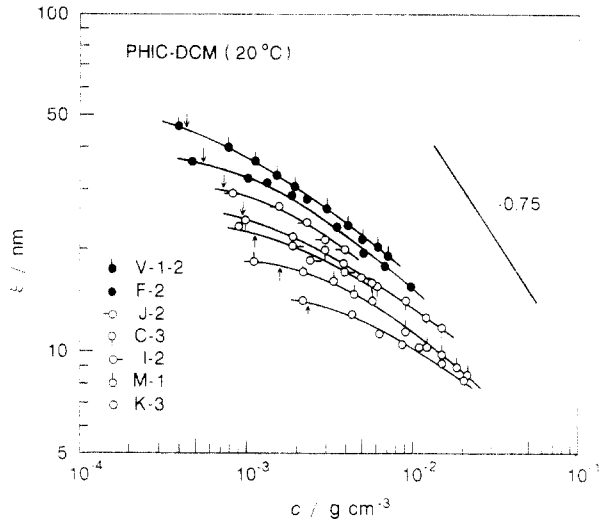

Figure 6. Concentration dependence of ξ for PHIC in DCM. The arrow indicates the overlap concentration c^* for each sample.

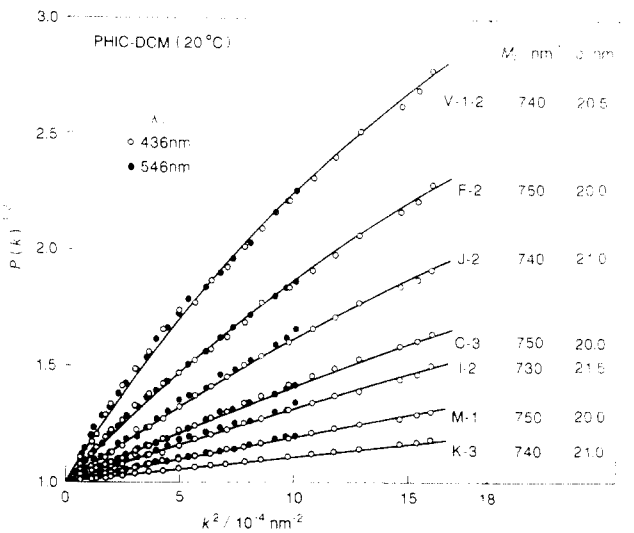

Figure 7. Comparison of the experimental intramolecular interference factor $P(k)$ for the seven PHIC samples in DCM with the Yoshizaki–Yamakawa theory[21] for the wormlike chain model.

The correlation length ξ can be obtained from the initial slope and intercept of the plot of $\hat{S}(k)^{-1/2}$ vs k^2 as shown in Figure 1 (cf. eq 2). Figure 6 shows the concentration dependence of ξ for PHIC in DCM in a double-logarithmic plot. The arrows in the figure indicate the overlap concentration c^* calculated from eq 3 for each sample. For flexible polymer–good solvent systems, the concentration dependence of ξ obeys the scaling law $\xi \propto c^{-3/4}$ in a c range slightly beyond c^*.[6,17] The concentration dependence of ξ for the PHIC–DCM system is much weaker than for the flexible polymer–good solvent systems in a similar c/c^* range. A similar weak concentration dependence of ξ was also reported by DeLong and Russo[9] for DMF solutions of PBLG, which is much stiffer than PHIC.

4. Discussion

4.1. Dilute Solution Data. Previously, Itou et al.[10] determined the wormlike chain parameters of PHIC in DCM from the analysis of their intrinsic viscosity data by the Yamakawa–Fujii–Yoshizaki theory.[18,19] The persistence length q and the molar mass per unit contour length M_L they obtained were 21 nm and 740 nm^{-1}, respectively. Using the same parameters, we can calculate $\langle S^2 \rangle^{1/2}$ from the Benoit–Doty equation[20] for the unperturbed wormlike chain model. The solid curve in Figure 4 for the DCM solution represents the theoretical results. The agreement between theory and experiment is very good. The solid curve fitting n-hexane solution data in the same figure was drawn using q = 42 nm and M_L = 715 nm^{-1}, which were determined by Murakami et al.[11] While the value of M_L is almost equal to that in DCM, q is twice larger than that in DCM. That is, the PHIC chain is more flexible in DCM than in n-hexane.

Figure 7 compares the intramolecular interference factor $P(k)$ [$\equiv \hat{S}(k)/(M_w/M_0)$ at infinite dilution] for the seven PHIC samples in DCM with the theoretical curves[21] of Yoshizaki and Yamakawa for unperturbed wormlike chains. To fit the experimental data points, we chose the values of the wormlike chain parameters written in the figure, all of which are close to those used to fit the $\langle S^2 \rangle^{1/2}$ data in Figure 4.

Using M_L = 740 nm^{-1} and q = 21 nm obtained above for PHIC in DCM, one can calculate the number of Kuhn statistical segments N for the PHIC samples used. The sixth column of Table 1 lists the results of N.

From the nice fittings of the $\langle S^2 \rangle^{1/2}$ and $P(k)$ data (as well as the $[\eta]$ data listed in the fifth column of Table 1 and of Itou et al.[10]) for PHIC in DCM by the theories for the unperturbed wormlike chain model, we can say that the intramolecular excluded volume effect is negligible for the PHIC chain in the good solvent DCM at least up to $M_w \leq 1.06 \times 10^6$ (or the Kuhn statistical segment number $N \leq 34.1$). This may be ascribed to the negligible probability of the collision among segments within one chain far separated along the chain contour. In Figure 4, the data points of $\langle S^2 \rangle^{1/2}$ for the two highest molecular weight samples in n-hexane slightly deviate upward from the theoretical curve. Murakami et al.[11] attributed this deviation to the intramolecular excluded volume effect.

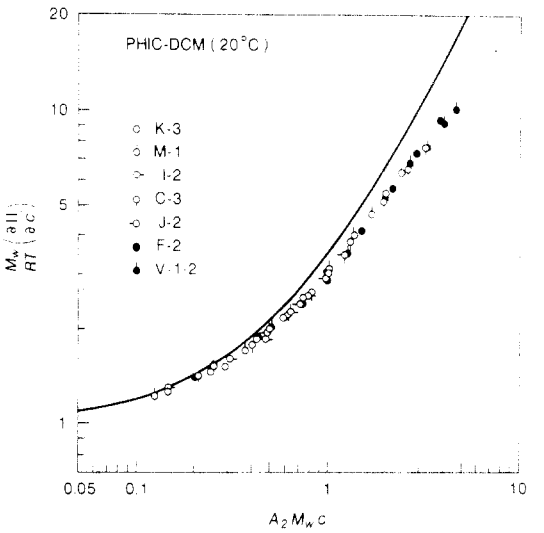

Figure 8. Double-logarithmic plot of $(M_w/RT)(\partial\Pi/\partial c)$ obtained from light scattering against A_2M_wc: curve, renormalization group theory of Ohta and Oono[3,6] for monodisperse fully flexible polymer–good solvent systems.

4.2. Osmotic Compressibility and Correlation Length Data. Figure 8 shows the double-logarithmic plot of $(M_w/RT)(\partial\Pi/\partial c)$ against A_2M_wc (the second virial term) for semidilute solutions of PHIC measured by light scattering. The data points for different molecular weight samples seem to follow a universal curve within the concentration range examined.[22] This behavior is similar to that of the flexible polymer–good solvent system.

The solid curve in Figure 8 represents the values of $(M/RT)(\partial\Pi/\partial c)$ obtained from the renormalization group

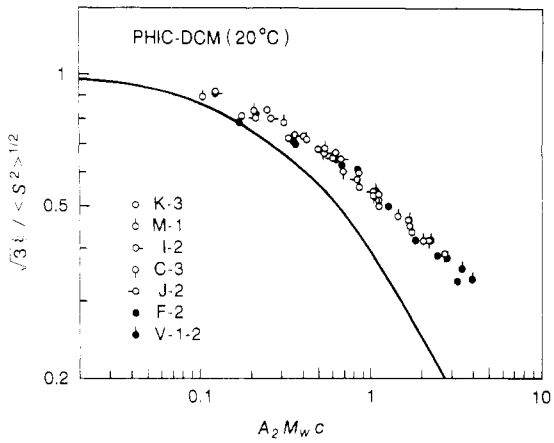

Figure 9. Double-logarithmic plot of $(3\xi^2/\langle S^2\rangle)^{1/2}$ vs A_2M_wc: curve, renormalization group theory of Ohta and Nakanishi[4,5] for fully flexible polymer–good solvent systems.

theory of Ohta and Oono[3,6] for (monodisperse) *fully flexible* polymers in a good solvent (M is the polymer molecular weight). This theoretical curve contains no adjustable parameters. As mentioned in the Introduction, this theory nicely agreed with experimental results of the osmotic compressibility for a flexible polymer in a good solvent.[6] However, the data points for PHIC in DCM do not follow this theoretical curve, exhibiting one of the differences between flexible and semiflexible polymers.

Figure 9 shows the double-logarithmic plot of $(3\xi^2/\langle S^2\rangle)^{1/2}$ vs A_2M_wc for semidilute solutions of PHIC. The data points for different molecular weight samples are almost scaled in this plot, like the flexible polymer–good solvent system, within the concentration range examined, but Ohta and Nakanishi's curve of the renormalization group theory[4,5] cannot fit the data points for the semiflexible polymer PHIC. The deviation is more enhanced in the correlation length than in the osmotic compressibility.

4.3. Comparison of the Osmotic Compressibility Data with the Scaled Particle Theory Including an Attractive Interaction. It has been shown that thermodynamic properties of many stiff-chain polymer solutions are favorably compared with the scaled particle theory for hard spherocylinder solutions.[13,23,24] The scaled particle theory for hard straight spherocylinder systems was first presented by Cotter,[25] and recently Sato et al.[24] showed that Cotter's result as it stands can be applicable to (isotropic) solutions of wormlike hard spherocylinders with sufficient stiffness.

The scaled particle theory can be generalized to polymer systems where polymers interact with each other not only by the hard-core repulsion but also by a weak attractive interaction. In this section, we briefly describe the scaled particle theory including a weak attractive interaction, and compare it with both $(\partial c/\partial\Pi)$ and the second virial coefficient of the PHIC–DCM system obtained above from light scattering and sedimentation equilibrium.

Let us consider an isotropic solution of wormlike spherocylinders. Each spherocylinder is assumed to have a hard-core diameter d and a contour length L_c of the cylinder part and also to interact with other spherocylinders by a weak attractive force; the potential u (of mean force) between two spherocylinders is written as

$$u = u_0 + w \tag{4}$$

where u_0 and w are the hard-core potential and attractive interaction potential, respectively, defined by

$$u_0 = \begin{cases} \infty & \text{when the hard cores of the two molecules overlap} \\ 0 & \text{otherwise} \end{cases} \tag{5}$$

$$w = \begin{cases} 0 & \text{when the hard cores of the two molecules overlap} \\ \text{finite} & \text{otherwise} \end{cases} \tag{6}$$

The osmotic pressure Π of the above solution can be formulated from a perturbation theory where the system with $u = u_0$ is taken as a reference system and the attractive interaction w is treated as a thermodynamic perturbation. Following our approach to this problem on an electrostatic interaction,[26] we use here the previously derived expression for $(\partial\Pi/\partial c)$

$$\frac{M}{RT}\left(\frac{\partial\Pi}{\partial c}\right) = \frac{M}{RT}\left(\frac{\partial\Pi}{\partial c}\right)_{u=u_0} - \langle\beta_w\rangle\frac{N_A}{M}c + \dots \tag{7}$$

where M is the molecular weight of the polymer. The first term is the osmotic pressure for the reference wormlike hard spherocylinder system ($u = u_0$) and the second term is the first-order perturbation term where $\langle\beta_w\rangle$ is the binary cluster integral with respect to w; $\langle\dots\rangle$ represents the average with respect to conformations and orientations of two interacting spherocylinders. If the attractive interaction is weak, the second and higher perturbation terms are not so important. In what follows, we neglect the higher order perturbation terms in eq 7.

The scaled particle theory for the wormlike hard spherocylinder gives[24,25]

$$\frac{M}{RT}\left(\frac{\partial\Pi}{\partial c}\right)_{u=u_0} = \frac{1}{(1-\nu c')^2}\left[1 + \frac{Bc'}{1-\nu c'} + \frac{2Cc'^2}{(1-\nu c')^2}\right] \tag{8}$$

Here ν is the molecular volume, c' is the number concentration of the polymer ($=cN_A/M$), and B and C are coefficients defined by

$$B = \frac{\pi}{2}L_c^2 d + 6\nu, \qquad C = \nu'\left(\frac{\pi}{2}L_c^2 d + 4\nu''\right) \tag{9}$$

where $\nu' \equiv \nu + (\pi/12)d^3$ and $\nu'' \equiv \nu - (\pi/24)d^3$.

As shown in the Appendix, the binary cluster integral $\langle\beta_w\rangle$ with respect to the attractive interaction for stiff-chain polymers may be written in the form

$$\langle\beta_w\rangle = -\frac{\pi}{2}L^2\bar{\delta} \tag{10}$$

where L is the contour length of the polymer ($=L_c + d$) and $\bar{\delta}$ is defined by eq A3. In this paper, we take $\bar{\delta}$ as an adjustable parameter without specifying the explicit form of w.

From eqs 7–10, the second virial coefficient A_2 and the reduced third virial coefficient g can be written as

$$A_2 = \frac{\pi N_A}{4M_L^2}[(d + \bar{\delta}) + d(X^{-1} + O(X^{-2}))] \tag{11}$$

and

$$g \equiv \frac{A_3}{A_2^2 M} = \frac{10}{3}X^{-1}(1 + \bar{\delta}/d)^{-2} + O(X^{-2}) \tag{12}$$

where X is the axial ratio ($=L/d$). The inverse propor-

tionality of the leading term of g to the polymer molecular weight for wormlike spherocylinders (eq 12) is distinct from the weak molecular weight dependence of g for flexible polymer–good solvent systems.[27,28] In the case of the long hard rod, the result of eq 12 is in good agreement with those obtained by Straley ($=12.3/3X$)[29] and Kihara ($=12/3X$).[30]

We first compare eq 11 with the experimental results of A_2. The contour lengths L estimated from M_w/M_L for all PHIC samples used in this study are longer than 150 nm (M_L = 740 nm^{-1}). Since the hard-core diameter of PHIC may be on the order of 1 nm, X^{-1} of the samples must be smaller than 10^{-2}. If we neglect the terms of the order of X^{-1} in eq 11 (which is justified by the molecular weight independence of A_2 shown in Figure 5), we can estimate the value of $d + \bar{\delta}$ to be 0.71 ± 0.02 nm from the experimental results of A_2 listed in Table 1.

The osmotic compressibility given by eqs 7–10 contains two unknown parameters d and $\bar{\delta}$. Fixing the value of $d + \bar{\delta}$ at 0.71 nm, we searched for d and $\bar{\delta}$ values leading to the best fit of all our data of the osmotic compressibility obtained from light scattering and sedimentation equilibrium to the scaled particle theory (eqs 7–11). Figure 10 demonstrates that the choice of d = 1.07 nm and $\bar{\delta}$ = −0.36 nm makes the theoretical lines fit very closely to the data points of $(M_0/RT)(\partial\Pi/\partial c)$ obtained in the present and previous studies.[31] Using the same values for d and $\bar{\delta}$, the reduced third virial coefficient g for sample C-3 is estimated to be 0.012 from eq 12. The result is close to the experimental value ($=0.01_5$). The value of d chosen is not very much different from the diameter of PHIC estimated from the partial specific volume[12] (=1.25 nm).

The good agreements in $(\partial\Pi/\partial c)$ at high concentrations and also in g between theory and experiment indicate that the higher perturbation terms (or the ternary and the higher cluster integrals including w) which were neglected in the theory do not appreciably contribute to the thermodynamic quantities of the PHIC–DCM system. Recently, van der Schoot and Odijk[32] calculated the third virial coefficient for rodlike polymers interacting with hard-core repulsive and soft attractive forces. Their result indicated that the attractive interaction part in the third virial term is significant provided the axial ratio of the rod is large enough. However, we cannot compare our result for the PHIC system with theirs as it stands, because PHIC is a semiflexible polymer. As pointed out by van der Schoot and Odijk, almost parallel configurations of three rods predominantly contribute to the attractive interaction part in the third virial term. Such configurations must be quite rare in the case of semiflexible polymers, and the contribution of the attractive third virial term to Π may be very much reduced by the polymer chain flexibility.

5. Conclusion

We undertook the light scattering and sedimentation equilibrium studies for the semiflexible polymer poly(*n*-hexyl isocyanate) (PHIC) dissolved in the good solvent dichloromethane (DCM) and found several characteristic features distinct from flexible polymer–good solvent systems as summarized below:

(1) The second virial coefficient is independent of the molecular weight.

(2) The reduced third virial coefficient is much smaller than that for flexible polymer–good solvent systems.

(3) A polymer chain with sufficient stiffness is not perturbed by the intramolecular excluded volume effect even in a good solvent.

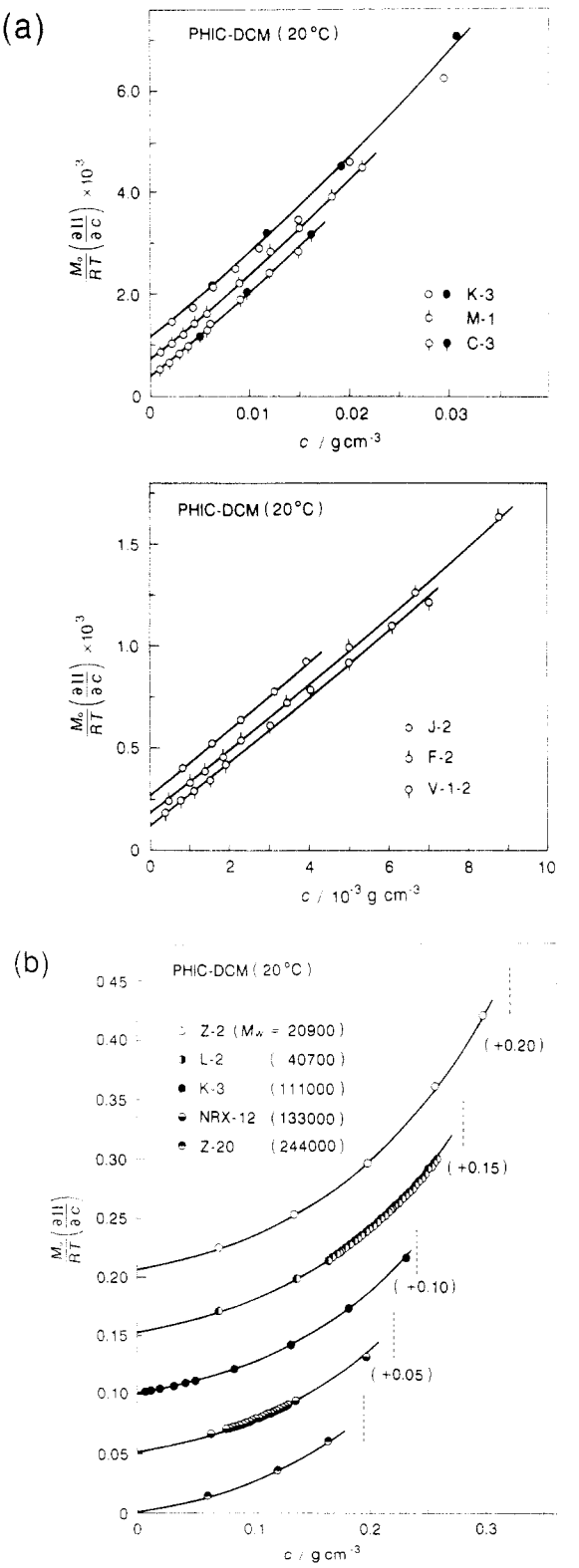

Figure 10. Comparison of the experimental results of $(M_0/RT) \times (\partial\Pi/\partial c)$ with the scaled particle theory containing a weak attractive interaction: (a) data obtained by light scattering (unfilled circles) and sedimentation equilibrium (filled circles) in the present study; (b) data over wide concentration ranges obtained from sedimentation equilibrium in the present (sample K-3) and previous[12] (the other samples) studies; theoretical curves, obtained from eqs 7–10 using d = 1.07 nm and $\bar{\delta}$ = −0.36 nm. In panel b, the data points and the theoretical curves except for sample Z-20 are shifted upward by the amount indicated in the parentheses, and the vertical dotted segments indicate the isotropic–nematic phase boundary concentration c_I.

(4) The osmotic compressibility in the semidilute regime does not obey the scaling law nor the renormalization group

theory applicable to flexible polymer–good solvent systems.

(5) The correlation length in the semidilute regime also does not obey the scaling law nor the renormalization group theory.

Features 1, 2, and 4 were properly explained by incorporating a weak attractive interaction into the scaled particle theory. (Here the scaled particle theory has nothing to do with the scaling arguments often applied to flexible polymer systems; see section 4.3.) Therefore we can say that this theory is useful for stiff-chain polymer–good solvent systems. The scaled particle theory itself cannot be used to discuss spatial properties of the solutions, such as the structure factor and the correlation length, because it is a thermodynamic theory. In a forthcoming paper, we propose an integral equation theory combined with the scaled particle theory to deal with the spatial properties.

Appendix: Expression of $\langle\beta_w\rangle$

In this appendix, we consider the binary cluster integral $\langle\beta_w\rangle$ with respect to the attractive interaction potential w for wormlike spherocylinders. This integral is defined by[26]

$$\langle\beta_w\rangle = \left\langle \frac{1}{V}\int\int\left[\exp\left(-\frac{w}{k_BT}\right)-1\right]d\mathbf{r}_{G1}\,d\mathbf{r}_{G2}\right\rangle \quad \text{(A1)}$$

where V is the volume of the system and $\mathbf{r}_{G1}$ and $\mathbf{r}_{G2}$ are the position vectors of the centers of mass of wormlike spherocylinders 1 and 2; $\langle\ldots\rangle$ represents the average with respect to conformations and orientations of the two spherocylinders. If the spherocylinder is nearly rodlike, i.e., if the Kuhn segment number N is small, the potential w should be a function of the distance r between the closest contour points, s_1 and s_2 on two interacting spherocylinders as well as the two unit tangent vectors $\mathbf{a}(s_1)$ and $\mathbf{a}(s_2)$ at the two contour points. Therefore it is convenient to specify the configuration of the two spherocylinders by s_1, s_2, r, $\mathbf{a}(s_1)$, and $\mathbf{a}(s_2)$ along with the position vector $\mathbf{r}_{G1}$ (or $\mathbf{r}_{G2}$) at given conformations of the two spherocylinders. (When two interacting spherocylinders are in a noncrossed configuration, where one or both of the closest contour points s_1 and s_2 are located at the spherocylinder end(s), the absolute value of w should be smaller than that in the case of the crossed configuration with the same r.[26] Here we approximate w for the noncrossed configuration to be zero and neglect the contribution of such configuration to $\langle\beta_w\rangle$.)

The parameters (s_1, s_2, r) can be regarded as curvilinear coordinates. The basis vectors of this coordinate system are $\mathbf{a}(s_1)$, $\mathbf{a}(s_2)$, and the unit vector $\mathbf{r}/r$, where $\mathbf{r}$ is the distance vector between the two contour points s_1 and s_2. The vector $\mathbf{r}/r$ is perpendicular to $\mathbf{a}(s_1)$ and $\mathbf{a}(s_2)$ (in the case of the crossed configuration), while the vectors $\mathbf{a}(s_1)$ and $\mathbf{a}(s_2)$ form the angle $\gamma(\mathbf{a}(s_1),\mathbf{a}(s_2))$. By using these coordinates, eq A1 can be rewritten in the form

$$\langle\beta_w\rangle \cong \left\langle 2\int_0^L ds_1\int_0^L ds_2\int_d^\infty dr\left|\sin\gamma(\mathbf{a}(s_1),\mathbf{a}(s_2))\right| \times \left[\exp\left(-\frac{w}{k_BT}\right)-1\right]\right\rangle = -\frac{\pi}{2}L^2\bar{\delta} \quad \text{(A2)}$$

where $L \equiv L_c + d$, $\bar{\delta}$ is defined by

$$\bar{\delta} \equiv \left\langle \frac{4}{\pi}\left|\sin\gamma(\mathbf{a}(s_1),\mathbf{a}(s_2))\right|\int_d^\infty\left[1-\exp\left(-\frac{w}{k_BT}\right)\right]dr\right\rangle \quad \text{(A3)}$$

and the approximate equality in eq A2 indicates that the contribution of the noncrossed configuration is neglected.

The parameter $\bar{\delta}$ is expected to be independent of L (or the molecular weight of the spherocylinder) if w is a short-range interaction potential, but it can depend on the degree of orientation in the system. We need an explicit expression of w to know the orientation dependence of $\bar{\delta}$.[32] Since the present study deals only with isotropic solutions, we take $\bar{\delta}$ as a phenomenological parameter in the text.

If the interaction range of w is much shorter than the persistence length q, the above discussion may be applied even to wormlike spherocylinders with considerably large N. This is because, in such a case, two or more pairs of contour points on two spherocylinders seldom come close within the interaction range of w instantaneously, and it is enough to consider only the case that two spherocylinders interact with each other at one pair of contour points along the two cylinders.

References and Notes

(1) de Gennes, P.-G. *Scaling Concepts in Polymer Physics*; Cornell University Press: Ithaca, NY, 1979.
(2) Doi, M.; Edwards, S. F. *The Theory of Polymer Dynamics*; Clarendon Press: Oxford, 1986.
(3) Ohta, T.; Oono, Y. *Phys. Lett.* **1982**, *89A*, 460.
(4) Ohta, T.; Nakanishi, A. *J. Phys. A: Math. Gen.* **1983**, *16*, 4155.
(5) Nakanishi, A.; Ohta, T. *J. Phys. A: Math. Gen.* **1985**, *18*, 127.
(6) Wiltzius, P.; Haller, H. R.; Cannell, D. S.; Schaefer, D. W. *Phys. Rev. Lett.* **1983**, *51*, 1183.
(7) Fujita, H. *Polymer Solutions*; Elsevier: Amsterdam, 1990; Chapter 2.
(8) Norisuye, T. *Prog. Polym. Sci.* **1993**, *18*, 543.
(9) DeLong, L. M.; Russo, P. S. *Macromolecules* **1991**, *24*, 6139.
(10) Itou, T.; Chikiri, H.; Teramoto, A.; Aharoni, S. M. *Polym. J.* **1988**, *20*, 143.
(11) Murakami, H.; Norisuye, T.; Fujita, H. *Macromolecules* **1980**, *13*, 345.
(12) Itou, T.; Sato, T.; Teramoto, A.; Aharoni, S. M. *Polym. J.* **1988**, *20*, 1049.
(13) Sato, T.; Teramoto, A. *Mol. Cryst. Liq. Cryst.* **1990**, *178*, 143.
(14) Sato, T.; Norisuye, T.; Fujita, H. *J. Polym. Sci., Part B: Polym. Phys.* **1987**, *25*, 1.
(15) Nakamura, Y.; Norisuye, T.; Teramoto, A. *J. Polym. Sci., Part B: Polym. Phys.* **1991**, *29*, 153.
(16) Noda, I.; Kato, N.; Kitano, T.; Nagasawa, M. *Macromolecules* **1981**, *14*, 668.
(17) Hamada, F.; Kinugasa, S.; Hayashi, H.; Nakajima, A. *Macromolecules* **1985**, *18*, 2290.
(18) Yamakawa, H.; Fujii, M. *Macromolecules* **1974**, *7*, 128.
(19) Yamakawa, H.; Yoshizaki, T. *Macromolecules* **1980**, *13*, 633.
(20) Benoit, H.; Doty, P. M. *J. Phys. Chem.* **1953**, *57*, 958.
(21) Yoshizaki, T.; Yamakawa, H. *Macromolecules* **1980**, *13*, 1518.
(22) It is noted that the data points of $(\partial\Pi/\partial c)$ at higher concentrations as shown in Figures 3 and 10b do not follow any universal curve in the plot of $(M_w/RT)(\partial\Pi/\partial c)$ vs A_2M_wc.
(23) Inatomi, S.; Sato, T.; Teramoto, A. *Macromolecules* **1992**, *25*, 5013.
(24) Sato, T.; Shoda, T.; Teramoto, A. *Macromolecules* **1994**, *27*, 164.
(25) Cotter, M. A. *J. Chem. Phys.* **1977**, *66*, 1098.
(26) Sato, T.; Teramoto, A. *Physica* **1991**, *A176*, 72.
(27) Norisuye, T.; Fujita, H. *Chemtracts Macromol. Chem.* **1991**, *2*, 293.
(28) Norisuye, T.; Nakamura, Y.; Akasaka, K. *Macromolecules* **1993**, *26*, 3791.
(29) Straley, J. P. *Mol. Cryst. Liq. Cryst.* **1973**, *24*, 7.
(30) Kihara, T., private communication.
(31) In the previous paper,[13] two of the authors (T.S. and A.T.) showed that $(\partial c/\partial\Pi)$ data of the PHIC–DCM system obtained from sedimentation equilibrium were favorably compared with the scaled particle theory for *hard* spherocylinder solutions using $d = 1.0$ nm (and $\bar{\delta} = 0$). This choice of the parameters gives the effective diameter $d + \bar{\delta}$ somewhat larger than 0.71 nm and cannot reproduce the A_2 nor $(\partial c/\partial\Pi)$ data as satisfactorily as the choice in the present study.
(32) van der Schoot, P.; Odijk, T. *J. Chem. Phys.* **1992**, *97*, 515.